

# DEVELOPING THE BEST CORRELATION FOR ESTIMATING THE TRANSFER OF OXYGEN FROM AIR TO WATER

WAYNE A. BROWN

McGill University • Montreal, Québec, Canada H3A 2B2

The study of engineering is usually carried out in a defined sequence. Students are first taught a set of basic tools that includes, for example, mathematical concepts and solution procedures along with the various conservation laws. They then apply these concepts to elementary problems associated with their chosen discipline. In the final stages of the educational process, the simple concepts are extended to allow the students to apply them to multifaceted engineering problems.

Due to the complexity of systems of practical interest, theory developed around simple systems cannot normally be applied in the form derived. Often the theory is used to identify the set of governing variables, and a relationship between these variables is then established empirically. To generalize these solutions over a number of experimental conditions, variables are often gathered into dimensionless groups. Although the number of independent dimensionless groups is governed by Buckingham's "Pi" theorem,<sup>[1]</sup> a number of useful groups have already been defined. These dimensionless groups represent ratios of competing effects, expressed in terms of experimental variables. Thus, development of an empirical relationship depends somewhat on the experience of the engineer or researcher. If particular effects are not identified as being important in the primary analysis, then they cannot be reflected in the final solution.

It is imperative that students be taught the following regarding problem analysis:

- ▶ *There are many different design equations that can be developed, depending on what assumptions are made. These assumptions are choices and are left to the judgment of the process engineer.*
- ▶ *The engineer should always use the applicable set of data to formulate a process design.*

- ▶ *More than one approach to a given problem may lead to a reasonable answer. The best approach is to consider many different methods of achieving a solution, but emphasis should be placed on the solution achieved by using the set of data most applicable to the problem at hand.*
- ▶ *It is often not possible to verify the results of an estimated parameter since a practical and accurate alternative measurement method may not exist. Thus, one may have to accept the results of an empirical correlation.*

We developed, and describe here, a laboratory exercise in an attempt to convey some of the above messages. It is based on the experimental determination of the overall mass-transfer coefficient describing the transfer of oxygen to water in an agitated tank.

## OBJECTIVES OF THE LABORATORY

The objectives of the laboratory exercise were to

- *Analyze a problem involving the transfer of oxygen to water and formulate a set of mathematical equations to adequately describe the process*
- *Fit the developed equations to experimental data to deter-*



**Wayne A. Brown** has held the position of Assistant Professor in the Department of Chemical Engineering at McGill University since 1999. Prior to that he worked for five years in the oil sand industry, first as a process engineer and then as a research scientist. He received his formal training at McGill, receiving his BEng (1989), MEng (1991), and PhD (1998) from the Department of Chemical Engineering.

**On a practical level, the lab deals with benign materials. As such, there are no fume hood requirements or disposal problems. The lab can easily be extended to examine the effect of other variables, such as temperature, oxygen partial pressure, and liquid volume.**

mine the mass-transfer coefficient

- Study the influence of the measuring device on estimates of the mass-transfer coefficient
- Develop the semi-empirical equations first put forth by Richards to estimate the mass-transfer coefficient
- Compare experimental results with estimates obtained from the Richards equation
- "Tailor" the Richards relation so that it makes the most use of the data collected

## EQUATION DEVELOPMENT

### Mass Transfer Coefficient from Experimental Data

The transfer of oxygen from a gas to a liquid phase can be divided into a number of transfer resistances.<sup>[2]</sup> The set of equations that describes the transfer of oxygen from a gas phase to water in a batch system is dependent on the assumptions applied. Some of the issues to be considered are:

- The change in concentration of oxygen in the air over the residence time in the liquid phase
- The transfer of inert components from the air, in addition to oxygen
- The composition of the particular gases used
- The change in gas holdup with time
- The mixing characteristics of the gas phase
- The mixing characteristics of the liquid phase
- The presence of additives in the liquid phase
- The change in volumetric gas flow rate due to the transfer of matter from the gas to liquid phases
- The resistance to mass transfer across the gas-liquid interface
- The influence of surface aeration

The implications of various assumptions on the resulting differential equations are discussed elsewhere.<sup>[3-9]</sup> For the current experimental setup, the following assumptions are assumed reasonable:

- There is negligible change in oxygen concentration in the gas phase.
- The gas holdup stays constant with time.
- The concentrations of oxygen in the gas and liquid phases are in equilibrium at the gas-liquid interface.
- The liquid is well mixed.

These assumptions lead to the following equations for the gas and liquid phases:

$$\frac{dC_L}{dt} = K_L a (C_L^* - C_L) \quad (1)$$

$$\frac{dC_G}{dt} = 0 \quad (2)$$

where  $K_L a$  is the volumetric mass-transfer coefficient.

These equations can be integrated subject to the initial conditions  $C_L(0) = 0$  and  $C_G(0) = C_G^0$  to yield

$$C_L(t) = C_L^* (1 - e^{-K_L a t}) \quad (3)$$

$$C_G(t) = C_G^0 \quad (4)$$

The problem is further complicated when the measurement method is considered in the analysis. One of the most common and convenient methods for measuring dissolved oxygen is through application of a dissolved oxygen electrode. To make a measurement, oxygen dissolved in the surrounding fluid must diffuse to the probe membrane, across the membrane, and finally through the probe solution to the active electrode tip. A number of approaches have been applied successfully to model this process, such as Fick's second law.<sup>[9]</sup> However, if the bulk solution in the tank is not viscous, transport through the electrode membrane can be treated as a first-order process, described by an equation of the form

$$\frac{dC_p}{dt} = \frac{1}{\tau_p} (C_L - C_p) \quad (5)$$

Here, the diffusion through the probe solution is neglected. Substituting Eq. (3) into Eq. (5) and integrating the result subject to the initial condition

$$C_p(0) = 0 \quad (6)$$

an expression relating the overall mass-transfer coefficient to the probe output can be derived

$$C_p(t) = C_L^* \left( 1 + \frac{K_L a}{k_p - K_L a} e^{-k_p t} - \frac{k_p}{k_p - K_L a} e^{-K_L a t} \right) \quad (7)$$

Using this equation, the overall liquid mass-transfer coefficient can be determined directly from the probe output. To determine the probe time constant, Eq. (5) is solved, subject to the conditions given by Eq. (6) and Eq. (8):

$$C_L(t) = C_L^* \quad (8)$$

In Eq. (8),  $C_L^*$  is a constant for a given oxygen partial

pressure and system temperature. Using Eqs. (6) and (8), Eq (5) can be integrated to yield

$$C_p(t) = C_L^* (1 - e^{-k_p t}) \quad (9)$$

### Generalized Correlation of Oxygen-Transfer Data

The volumetric mass-transfer coefficient,  $K_L a$  is a complex function, dependent on the system geometry, the properties of the liquid, and the process operating conditions. In terms of basic variables, the function can be expressed as

$$K_L a = K_L a(d_i, n_i, h_i, w_i, l_i, d_T, h_L, n_B, w_B, \rho_f, \mu_f, \sigma_f, D_{O_2}, N, v_S, v_t, g) \quad (10)$$

In developing his correlation, Richards considered  $K_L$  and "a" separately. For geometrically similar vessels, dimensionless groups related to geometry do not vary. In this particular situation, the overall mass-transfer coefficient per unit transfer area,  $K_L$ , associated with the transfer of oxygen from a gas phase to a Newtonian fluid is expected to be a function of the variables

$$K_L = \text{fn}(N, d_i, \rho_f, \mu_f, D_{O_2}) \quad (11)$$

From Buckingham's Pi theorem, three dimensionless groups can be created. Thus, as suggested by Rushton,<sup>[10]</sup> the relationship can be written

$$\frac{K_L d}{D_{O_2}} = K_1 \left( \frac{N d_i^2 \rho_f}{\mu_f} \right)^\alpha \left( \frac{\mu_f}{D_{O_2} \rho_f} \right)^\beta \quad (12)$$

Here,  $K_1$  is a constant that accounts for the geometry of the particular system. For convective mass transfer between spherical particles and a liquid,  $\alpha$  has been shown empirically to have a value in the range of  $0.4 \leq \alpha \leq 0.6$ .<sup>[11]</sup> In his derivation, Richards used a value of  $\alpha = 0.5$ . Thus, for constant diffusivity and fluid properties, and assuming that the gas consists of spherical bubbles, Eq. (12) reduces to

$$K_L = K_2 N^{0.5} \quad (13)$$

Richards' development is completed by noting that the interfacial area for mass transfer is correlated adequately by Calderbank's equation<sup>[11]</sup>

$$a = K_3 \left[ \frac{(P_G / V_L)^{0.4} \rho_L}{\sigma_L} \right] \left[ \frac{v_S}{v_t} \right]^{0.5} \quad (14)$$

As shown through the dimensional analysis performed by Rushton, *et al.*,  $P_G$  is itself a function of a subset of the variables introduced in Eq. (10).<sup>[12]</sup> For the assumption of constant fluid properties applied above, the Richards correlation for the overall mass transfer coefficient is obtained by multiplying Eqs. (13) and (14) to yield

$$K_L a = K_4 (P_G / V_L)^{0.4} v_S^{0.5} N^{0.5} \quad (15)$$

Data from a number of different systems have been correlated

using the relation developed by Richards.<sup>[13,14]</sup>

In applying the Richards equation, data on the power requirements of the gassed system are not always readily available. Therefore, as part of the current development, it is useful to express the correlation in terms of the more commonly measured variables as they appear in Eq. (10). Useful for this purpose is the empirical correlation put forth by Michel, *et al.*,<sup>[15]</sup>

$$P_G = K_5 \left( \frac{P^2 N d_i^3}{Q^{0.56}} \right)^{0.45} \quad (16)$$

Note that this equation is not dimensionless, and thus care should be taken when extrapolating outside the range in which the data was collected. An estimate of the *ungassed* power requirements can be obtained from the dimensionless relationship based on the Rushton's power number.<sup>[12]</sup> For geometrically similar vessels, function is of the form

$$Po = \frac{P}{N^3 d_i^5 \rho_f} = K_6 \left( \frac{d_i^2 N \rho_f}{\mu_f} \right)^\gamma \left( \frac{d_i N^2}{g} \right)^\lambda = \text{fn}(\text{Re}, \text{Fr}) \quad (17)$$

The Froude number (Fr) is only important if a vortex is formed. As most systems are baffled, the dependence of the power number (Po) on Fr is usually not considered, and Eq. (17) reduces to a function of Re only. This function is often expressed graphically. Since the dimensionless groups

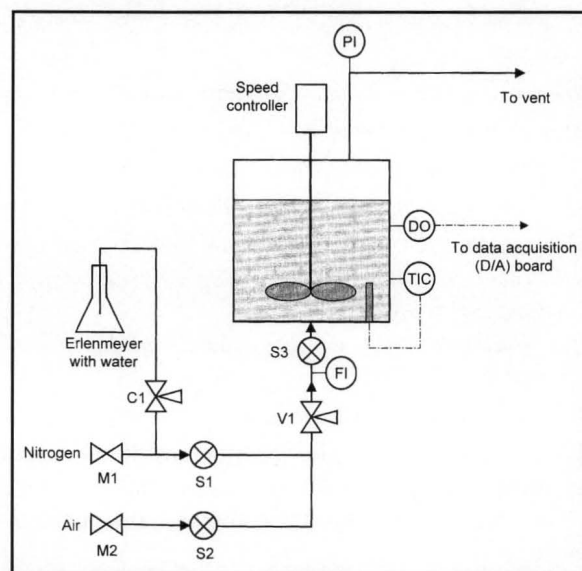


**Figure 1.** Experimental apparatus. Temperature (TI), pressure (PI), gas flow rate (FI), and dissolved oxygen (DO), were measured continuously. Only the signal from the dissolved oxygen probe was sampled by the data acquisition board, however. Solenoid valves S1, S2, and S3 were used to choose the source of the gas added to the fermenter, while valve V1 was used to adjust the flow rate. Valve C1 was used to purge the Erlenmeyer flask with nitrogen for determination of the probe time constant. Details of the procedure can be found in the text.

related to geometry have not been included, however, a single curve for each impeller configuration is required. Thus, using Eqs. (15) through (17), an estimate of the mass-transfer coefficient can be obtained.

## EXPERIMENTAL

### Apparatus

A 4-L tank was used for all experiments (see Figure 1). The vessel was 13 cm in diameter and had a height of 30 cm. No baffles were installed. All experiments were performed using 2 L of distilled water, resulting in a liquid depth of approximately 15 cm. A flat-blade propeller was used that was 6.5 cm in diameter from tip to tip. The propeller had 4 blades and was located 2 cm from the bottom of the vessel. Air was introduced into the bottom of the tank through a sparger that consisted of four equally spaced holes, directed radially outward. The temperature was controlled by means of a 300-W heater connected to a controller (Omega Model BS5001J1). Dissolved oxygen was measured using a dissolved oxygen electrode (Ingold DL-531) in conjunction with a digital meter equipped with an analog output (Cole-Parmer Model 01971-00). Data from the meter was logged on a personal computer by means of a data-acquisition board and bundled data-acquisition software (LABTECH notebook for Windows).

Experiments were run over a range of gas flowrates (2-4 L min<sup>-1</sup>) and stirring speeds (100-1200 rev min<sup>-1</sup>). Prior to each set of experiments, the probe was calibrated using nitrogen and oxygen saturated solutions of water. All experiments were performed at 30°C and at atmospheric pressure.

### Determination of Probe Time Constant

The dissolved oxygen probe was placed into a flask of

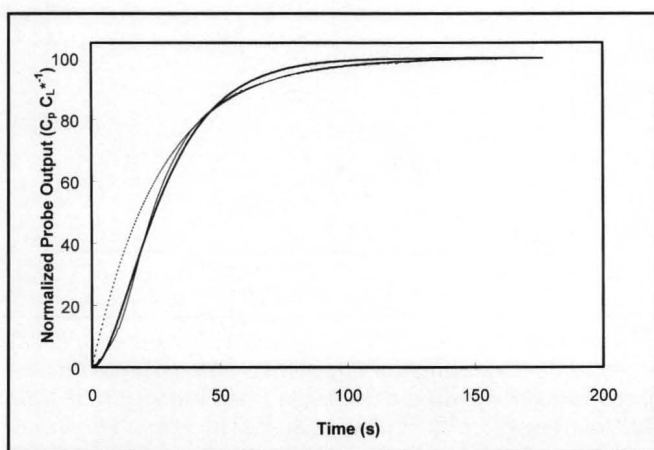


**Figure 2.** Fit of Eq. (3) (dotted line) and Eq. (7) (thick solid line) to experimental data (thin solid line). Experimental data were generated at an air flowrate of 3 L min<sup>-1</sup> and a stirring speed of 1100 rev min<sup>-1</sup>. In calculating  $K_L a$  by Eq. (3), only data between 30 and 98% saturation were considered, as described in the text.

Spring 2001

water that had been purged to saturation with nitrogen (see Figure 1). After a reading of 0% had been established, the probe was quickly immersed into the vessel containing 2 L of water saturated with oxygen to 100%. Under these conditions, the dynamics of the probe are described by Eqs. (5), (6), and (8). To facilitate the determination of the probe constant, a linearized form of Eq. (9)

$$\ln\left(\frac{C_L^*}{C_L^* - C_p}\right) = k_p t \quad (18)$$

was used. From Eq. (18), a plot of  $\ln\left(C_L^* / (C_L^* - C_p)\right)$  versus  $t$  should yield a straight line with a slope of  $k_p$ . The slope of the best-fit line was determined by linear regression.

### Determination of $K_L a$

The vessel was first purged with nitrogen until the dissolved oxygen probe stabilized at a value of 0%. The purge gas was then switched instantaneously to air through means of a series of solenoid valves (see Figure 1). An estimate of the mass-transfer coefficient was then obtained by fitting Eq. (7) to the data collected. As the model function cannot be linearized, a nonlinear regression algorithm was used to extract the best estimate of  $K_L a$  from each data set.

## RESULTS AND DISCUSSION

As a preliminary exercise to the laboratory, students were asked to develop the appropriate equations with which to estimate  $K_L a$ . It became apparent to the students during this exercise that the set of equations generated depends on the assumptions that were made with respect to specific aspects of the problem. For instance, if it was assumed that the rate of mass transfer from the gas to liquid is small compared to the dynamic associated with the probe, then  $(1 / K_L a) \gg \tau_p$ , and the effect of the probe is negligible. Under these circumstances, the rate of mass transfer can be calculated adequately from Eq. (3); but if this is not the case, then the probe dynamics must be taken into account.<sup>[16]</sup> Thus, a function such as Eq. (7) is required.

The probe constant was calculated by each group of students using a graphical approach. Typical values obtained for  $\tau_p$  were between 14 and 17 s. From Eq. (5) the probe output should attain a value of 63% saturation when  $t = \tau_p$ . From the experimental data used to determine  $\tau_p$ , this condition was verified (data not shown). Therefore, Eq. (5) proved to be an adequate representation of the dynamics of the probe.

Typical data obtained by the students for calculation of  $K_L a$  is shown in Figure 2. It has been shown that truncating data collected early in the experiment can minimize the effect of the probe on the estimate of  $K_L a$ .<sup>[17]</sup> Therefore, under appropriate conditions, reasonable estimates of  $K_L a$  can be obtained from Eq. (3) and knowledge of the probe dynamics is not required. Even when these conditions are



met, however, due to the exponential nature of Eq. (3) the best estimates of  $K_L a$  are obtained from Eq. (3) using data collected at times on the order of the time constant,  $\tau=1/K_L a$ . As such, it is recommended that data above 30% saturation never be discarded.<sup>[17]</sup>

For the current exercise, when neglecting the effect of the probe, only data between 30 and 98% saturation were considered when determining  $K_L a$  using Eq. (3). When the probe dynamics were considered, however, Eq. (7) was applied and all of the data collected were used. Using the data shown in Figure 2, Eq. (3) and Eq. (7) yield  $K_L a$  estimates of  $134 \text{ h}^{-1}$  and  $285 \text{ h}^{-1}$ , respectively. Therefore, serious errors result if the probe dynamics are not considered. This is to be expected since the dynamics of the mass-transfer process and the probe are on the same order for these data. Thus, the concept that the measuring device is an integral part of a process is reinforced.

From Figure 2 it is apparent that Eq. (7) adequately represents the data, where Eq. (3) does not. In addition, for two first-order processes in series, the sum of the time constants of each process should equal the time at which the overall process achieves a value of 63%. For the data presented, a value of 63% is achieved at approximately 30 s. The sum of the time constants,  $\tau_p + 1/K_L a$ , is equal to 29 s. Therefore, the assumptions that led to the development of Eq. (7) appear to be appropriate—other formulations could also fit the data as well or possibly even better, however. For instance, unsteady-state diffusion to the active element in the probe could have been solved using the appropriate form of the diffusion equation.<sup>[7]</sup> The solution to this problem can then be fit to the data to determine the probe time constant.

The range over which the dynamics of the probe can be neglected was studied by comparing estimates of  $K_L a$  obtained using Eqs. (3) and (7) (see Figure 3). From this figure, it can be seen that the two estimates deviate at relatively low values of  $K_L a$ . Quantitatively, it is apparent that the impact of the probe becomes important when the probe time constant is 20% of the time constant associated with the transfer process,  $1/K_L a$ . This “rule of thumb” has also been suggested by others.<sup>[17]</sup>

The data generated by the students was then compared with the Richards equation. This was accomplished by plotting the  $K_L a$  estimates obtained by the students on the same axes as the data used to generate the relationship in the original work by Richards (see Figure 4). When originally presented,  $K_L a$  was quoted in units of  $\text{mML}^{-1}\text{h}^{-1}\text{atm}^{-1}$ .<sup>[13]</sup> This selection of units was most probably related to the sodium sulphite oxidation method that was used to generate the data. Data generated using this technique are often displayed as  $H'K_L a$ , where  $H'$  is Henry's constant.<sup>[18]</sup> To facilitate comparison with the data generated by the students, data used to generate the original correlation were divided by Henry's constant at  $30^\circ\text{C}$  (see Figure 4). In the laboratory exercise,

axes complete with the data used by Richards were handed out in printed form to each lab group. Thus, the comparison exercise necessitated that the points be plotted by hand. Therefore, the students were forced to critically examine the deviation of the experimental values from the Richards equation. The data generated scatters within the bounds of the original data sets. This scatter is rather large, however. For instance,  $K_L a$  values of between 75 and  $250 \text{ h}^{-1}$  correspond to a value of 300 on the abscissa. Thus, estimates by the corre-

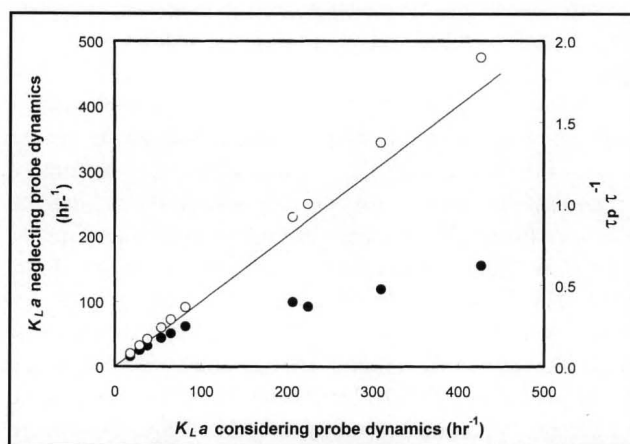


**Figure 3.** Comparison of estimates of  $K_L a$  obtained by considering (Eq. 7) and neglecting (Eq. 3) the probe dynamics. Closed circles represent the  $K_L a$  estimates, while open circles represent the ratio of the probe time constant to the time constant of the transfer process, where  $\tau=1/K_L a$ . The solid line indicates a perfect correspondence between the two estimates of  $K_L a$ .

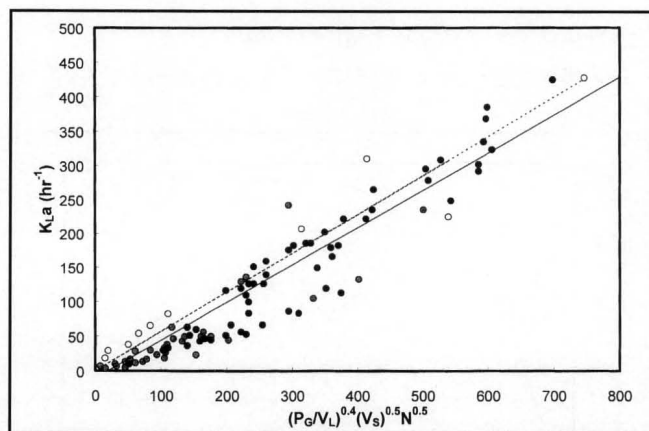


**Figure 4.** Assessment of the applicability of the Richards equation to experimental apparatus. The ordinate has the units indicated, while the abscissa has units of  $(\text{HP}/1000 \text{ L})^{0.4}(\text{cm}/\text{min})^{0.5}(\text{RPM})^{0.5}$ . Black (Richards<sup>[13]</sup>) and gray (Cooper<sup>[18]</sup>) circles represent the data originally used by Richards to assess his correlation. Results were divided by Henry's constant at  $30^\circ\text{C}$ , as described in the text. The solid line represents the best fit to these data, as suggested by Richards. Open circles represent data generated as part of the current laboratory exercise. The dotted line represents the results of Eq. (19).

lation are on the order of  $\pm 50\%$ . This finding is often difficult for many students to accept, as critical analysis of empirical correlations on this level is new for them.

The correlation developed by Richards underestimates the data generated by the students in almost all of the cases (Figure 4). There are two plausible explanations for this result. First, the original development of the correlation was meant to apply to geometrically similar vessels.<sup>[13]</sup> Therefore, it is possible that the consistent offset from the Richards correlation is related to geometric differences between the systems used to generate the various data sets.

The Richards equation can be tuned for a specific geometry as follows: For the experimental system at hand, only  $N$  and  $Q$  are varied; furthermore, for Reynolds numbers associated with all stirring speeds, it can be shown that  $Po$  is constant in Eq. (17).<sup>[14]</sup> Thus, Eqs. (15) through (17) can be reduced to

$$K_L a = K_7 N^{1.76} Q^{0.4} \quad (19)$$

This equation has one adjustable parameter ( $K_7$ ) that accounts for geometry and the fluid properties of the system. As a first step to improving the correlation,  $K_7$  was determined using only the student data. The resulting equation was plotted on Figure 4. Because only data specific to the system under study was used, Eq. (19) is a better representation of the system used in the study, as is evident in the superior fit.

A second plausible explanation to account for the differences noted between the Richards correlation and the experimental data is related to surface effects. In its development, the Richards correlation assumes that the tanks are well

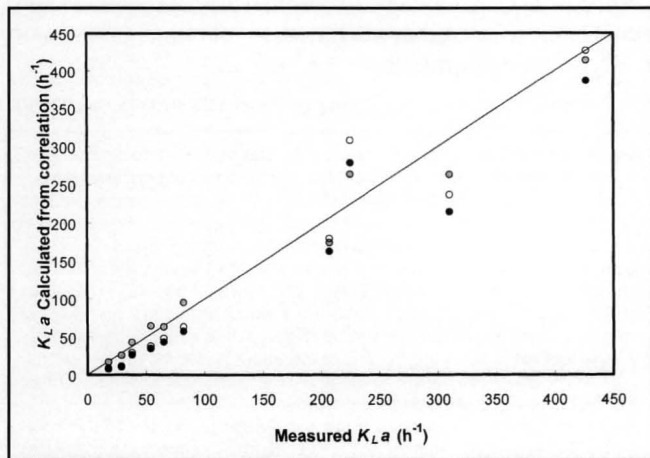


**Figure 5.** Ability of various correlation equations to fit the experimental data. Black circles represent results of the Richards correlation as originally presented (Eq. 15). Open circles represent the Richards correlation tailored for the geometry of the experimental system (Eq. 19). Grey circles represent the equation resulting when surface effects are considered through inclusion of the Froude number (Eq. 22).

baffled.<sup>[13]</sup> As a result, surface effects are negligible and no dependence on the Froude number is expected. The Froude number was also not considered in application of Eq. (17) for the same reason. The experimental apparatus used by the students had no baffles. Thus, a dependence of the  $K_L a$  on the Froude number is expected, especially for larger values of  $N$ .

To address this shortcoming in the original derivation, the Richards correlation is further modified to account for possible surface effects. The Froude number is defined as

$$Fr = \left( \frac{d_i N^2}{g} \right) \quad (20)$$

The desired equation can be obtained from Eqs. (19) and (20), and has the general form of

$$K_L a = K_7 \left( \frac{d_i}{g} \right)^\lambda N^{2\lambda+1.76} Q^{0.4} \quad (21)$$

Although the value of  $\lambda$  is not known, it is recognized that Eq. (21) is also a function of  $N$  and  $Q$  only. The specific value of  $\lambda$  could be determined through regression using the experimental data collected. In the resulting equation, the exponent of  $N$  would be tailored to the data collected by the students, while the functionality of  $Q$  would be dictated by the data sets originally used by Richards. Therefore, a more reasonable approach is to tailor *all* exponents to the experimental data generated by the students. The result of this exercise is the equation

$$K_L a = K_8 N^{1.35} Q^{0.60} \quad (22)$$

The ability of this equation to capture the relevant features of the experiment is readily seen in Figure 5. While the Richards equation represents the data well, the best fit results when the equation is tailored to the experimental data collected. Thus, while an adjusted correlation coefficient,  $r^2$ , of 0.81 is associated with the fit of Eq. (19), this value increases to 0.98 when Eq. (22) is applied. This result may seem obvious, as Eq. (22) has three adjustable parameters, while it appears as if Eq. (19) has only one. In actuality, however, both equations have three adjustable parameters. The difference is that the exponents in Eq. (19) were obtained from correlations fit using other sets of data, while those in Eq. (22) were fit to the data obtained with the current system only.

The difference among the three approaches becomes readily apparent at this point. As the equations are further tailored to the experimental data, the mathematical form better fits the data. Thus, the spectrum of possibilities associated with process design can be elucidated. When no data are available, the engineer must rely heavily on data generated from dimensionally similar systems. This approach is only justified, however, in the absence of reliable data associated with the system of interest. As data become available, the pre-

Continued on page 147.

# Estimating the Transfer of Oxygen

Continued from page 139.

ferred approach is to tailor the functional form derived from existing correlations in an attempt to maximize the use of the specific information available.

The laboratory exercise also has secondary benefits. First, the exercise bridges the gap between biotechnology and classical chemical engineering. Students are often under the impression that the area of biotechnology represents a radical departure from the chemical engineering principles applied to other industries. This laboratory serves to demonstrate that the "high tech" fields have been developed on the same set of principles as the mature industries. On a practical level, the lab deals with benign materials. As such, there are no fume hood requirements or disposal problems. The lab can easily be extended to examine the effect of other variables, such as temperature, oxygen partial pressure, and liquid volume.

## CONCLUSIONS

When faced with a design problem, the chemical engineer often must turn to empirical expressions, generalized through the application of dimensionless groups. But as data become available that are specific to the system of interest, the basic proven empirical expression should be tailored to reflect these data. Extracting the relevant parameters of interest (*i.e.*,  $K_L a$ ) from experimental data generated for this purpose is subjective, based heavily on the assumptions made by the engineer. Although many approaches may be adequate, others may lead to erroneous results. A key variable to consider when analyzing the problem is the influence of the measuring element on the resulting data set.

## NOMENCLATURE

$a$	area available for mass transfer per unit volume of ungasged liquid ( $\text{m}^2\text{m}^{-3}$ )
$C_G$	concentration of oxygen in the gas phase ( $\text{mol L}^{-1}$ )
$C_G^0$	concentration of oxygen in the gas phase at $t=0$ ( $\text{mol L}^{-1}$ )
$C_L$	concentration of oxygen in the liquid ( $\text{mol L}^{-1}$ )
$C_L^*$	concentration of oxygen in the liquid in equilibrium with the gas phase ( $\text{mol L}^{-1}$ )
$C_p$	concentration of oxygen in the liquid, as measured by the dissolved oxygen probe ( $\text{mol L}^{-1}$ )
$d_i$	impeller diameter (m)
$d_T$	tank diameter (m)
$D_{O_2}$	diffusivity of oxygen in water ( $\text{m}^2\text{s}^{-1}$ )
$g$	acceleration of gravity ( $\text{m s}^{-2}$ )
$h_i$	height of impeller from bottom of tank (m)
$h_L$	height of liquid (m)
$l_i$	length of impeller blades (m)
$H^2$	Henry's constant for oxygen and water ( $\text{mmol L}^{-1} \text{atm}^{-1}$ )
$K_1$	empirical constant
$K_L$	overall mass-transfer coefficient per unit transfer area,

	based on the liquid phase ( $\text{m s}^{-1}$ )
$K_L a$	volumetric mass-transfer coefficient, based on the liquid volume ( $\text{hr}^{-1}$ )
$k_p$	$(1 / \tau_p)(\text{s}^{-1})$
$n_B$	number of baffles
$n_i$	number of blades on impeller
$N$	stirring speed ( $\text{rev s}^{-1}$ )
$P$	power input into ungasged liquid (W)
$P_G$	power input into gasged liquid (W)
$v_s$	superficial gas velocity, based on cross section of vessel ( $\text{m s}^{-1}$ )
$v_t$	terminal rise velocity of a gas bubble ( $\text{m s}^{-1}$ )
$w_B$	width of baffles (m)
$w_i$	width of impeller blades (m)
$Q$	gas flow rate ( $\text{L s}^{-1}$ )
$t$	time (s)

## Greek symbols

$\alpha, \beta, \gamma, \lambda$	exponents in Eqs. (12), (17), and (21)
$\tau_p$	time constant of the dissolved oxygen probe (s)
$\tau$	time constant of the transfer process ( $1/K_L a$ )(s)
$\mu_f$	liquid viscosity (cp)
$\rho_f$	liquid density ( $\text{kg m}^{-3}$ )
$\sigma_f$	surface tension at gas-liquid interface ( $\text{mN m}^{-1}$ )

## REFERENCES

1. Geankoplis, C.J., *Transport Processes and Unit Operations*, Prentice-Hall, Inc., NJ (1993)
2. Bailey, J.E., and D.F. Ollis, *Biochemical Engineering Fundamentals*, 2nd ed., McGraw-Hill, Inc., New York, NY (1986)
3. Linek, V., J. Sinkule, and P. Benes, *Biotechnol. Bioeng.*, **38**, 323 (1990)
4. Linek, V., V. Vacek, and P. Benes, *Chem. Eng. J.*, **34**, 11 (1987)
5. Benedek, A., and W.J. Heideger, *Biotechnol. Bioeng.*, **13**, 663 (1971)
6. Sheppard, J.D., and D.G. Cooper, *J. Chem. Tech. Biotechnol.*, **48**, 325 (1990)
7. Ruchti, G., I.J. Dunn, and J.R. Bourne, *Biotechnol. Bioeng.*, **23**, 277 (1981)
8. Chang, H.N., B. Halard, and M. Moo-Young, *Biotechnol. Bioeng.*, **34**, 1147 (1991)
9. Wernau, W.C., and C.R. Wilke, *Biotechnol. Bioeng.*, **25**, 571 (1973)
10. Rushton, J.H., *Chem. Eng. Prog.*, **47**, 485 (1951)
11. Calderbank, P.H., *Trans. Instn. Chem. Engrs.*, London, **36**, 443 (1958)
12. Rushton, J.H., E.W. Costich, and H.J. Everett, *Chem. Eng. Prog.*, **26**, 395 (1950)
13. Richards, J.W., *Prog. Ind. Microbiol.*, **3**, 143 (1961)
14. Kargi, F., and M. Moo-Young, in Vol 2 of *The Principles of Biotechnology, Engineering Considerations*, C.O. Cooney and A.E. Humphrey, eds; in *Comprehensive Biotechnology: The Principles Applications and Regulations of Biotechnology in Industry, Agriculture and Medicine*, M. Moo-Young, ed., Pergamon Press, New York, NY
15. Michel, B.J., and S.A. Miller, *AIChE J.*, 262 (1962)
16. Tribe, L.A., C.L. Briens, and A. Margaritis, *Biotechnol. Bioeng.*, **46**, 388 (1994)
17. Merchuk, J.C., S. Yona, M.H. Siegel, and A.B. Zvi, *Biotechnol. Bioeng.*, **35**, 1161 (1990)
18. Cooper, C.M., G.A. Fernstrom, and S.A. Miller, *Ind. Eng. Chem.*, **36**, 504 (1944) □